Title

Nitrogen fate during agricultural managed aquifer recharge: Linking plant response, hydrologic, and geochemical processes

Authors

Levintal, Elad
Huang, Laibin
Prieto García, Cristina
et al.

Publication Date

2023-03-01

DOI

10.1016/j.scitotenv.2022.161206

Peer reviewed

Nitrogen fate during agricultural managed aquifer recharge: linking plant response, hydrologic, and geochemical processes

Elad Levintal[1], Laibin Huang[1], Cristina Prieto García[1], Adolfo Coyotl[1], Matthew W. Fidelibus[2], William R. Horwath[1], Jorge L. Mazza Rodrigues[1,3], Helen E. Dahlke[1,*]

1. Department of Land, Air and Water Resources, University of California, Davis, CA 95616, USA

2. Department of Viticulture and Enology, University of California, Davis, 1 Shields Ave., Davis, CA 95616, USA

3. Environmental Genomics and Systems Biology Division, Lawrence Berkeley National Laboratory, Berkeley, CA 94720, USA

* Corresponding author. E-mail address: hdahlke@ucdavis.edu (H.E. Dahlke)

Abstract

Agricultural managed aquifer recharge (Ag-MAR, on-farm recharge), where farmland is flooded with excess surface water to intentionally recharge groundwater, has received increasing attention by policy makers and researchers in recent years. However, there remain concerns about the potential for Ag-MAR to exacerbate nitrate (NO_3^-) contamination of groundwater, and additional risks, such as greenhouse gas emissions and crop tolerance to prolonged flooding. Here, we conducted a large-scale, replicated winter groundwater recharge experiment to quantify the effect of Ag-MAR on soil N biogeochemical transformations, potential NO_3^- leaching to groundwater, soil physico-chemical conditions, and crop yield. The field experiment was conducted in two grapevine vineyards in the Central Valley of California, which were each flooded for 2 weeks and 4 weeks, respectively, with 1.31 and 1.32 m^3 m^{-2} of water. Hydrologic, geochemical, and microbial results indicate that NO_3^- leaching from the first 1 m of the vadose zone was the dominant N loss pathway during flooding. Based on pore water sample and N_2O emission data denitrification played a lesser role in decreasing NO_3^- in the root zone but prolonged anoxic conditions resulted in a significant 29% yield decrease in the 4-week flooded vineyard. The results from this research, combined with data from previous studies, are summarized in a new conceptual model for integrated water-N dynamics under Ag-MAR. The proposed model can be used to determine best Ag-MAR management practices.

Keywords: MAR, groundwater recharge, nitrate, denitrification, soil, crop tolerance

1. Introduction

One-quarter of the world's population and 40% of agricultural production relies on overdrafted groundwater sources (Connor, 2015), with an expected increase in groundwater reliance due to climate change and growing water demand (Gorelick and Zheng, 2015; Haddeland et al., 2014; Siebert et al., 2010; Wada et al., 2010). Thus, reducing pressure on overdrafted groundwater systems is crucial to increase global resilience of food and drinking water in response to growing human population and climate change pressures.

Agricultural managed aquifer recharge (Ag-MAR, or on-farm recharge) is a form of managed aquifer recharge (MAR) where farmland is flooded with excess surface water to recharge groundwater intentionally (Grinshpan et al., 2021; Kocis and Dahlke, 2017; Waterhouse et al., 2020) and it has been increasingly used across the globe to address groundwater overdraft (Dillon et al., 2019; Levintal et al., 2022). The purpose of Ag-MAR, in comparison to more traditional MAR methods, is to transfer large amounts of surplus surface water from rivers or reservoirs to agricultural land (e.g., idle land, agricultural fields and orchards) that serve as spreading grounds for the recharge (Dahlke et al., 2018).

Ag-MAR adoption has increased in recent years, particularly in the USA and Europe (Grinshpan et al., 2021; Negri et al., 2020; Niswonger et al., 2017). In California, for example, Ag-MAR is implemented as one of the methods to overcome ongoing groundwater depletion (Kocis and Dahlke, 2017). However, using farmland as spreading grounds bears the risk to leach contaminants from the water or soil to groundwater which can impact drinking water quality (Bachand et al., 2014), waterlogging of the root zone for long periods that can reduce crop health

(Ganot and Dahlke, 2021a), and ecosystem service tradeoffs, such as short and long-term effects on in-stream flows (Levintal et al., 2022). Out of the above, leaching of legacy nitrogen (N), mainly in the form of nitrate (NO_3^-), is possibly the most widespread environmental risk of Ag-MAR. Consumption of drinking water above the maximum contaminant level (MCL; 10 mg L^{-1} NO_3^--N in California) can increase the risk of cancers, birth defects, and other adverse health effects (Weitzman et al., 2022). Globally, nitrate is the primary nonpoint source pollutant of groundwater (Beganskas et al., 2018; Bishayee et al., 2022; Richa et al., 2022), whereby agricultural lands serve as the main source for NO_3^- due to the buildup of legacy NO_3^- resulting from years of fertilizer use inefficiencies (Van Meter et al., 2016; Waterhouse et al., 2020).

In comparison to the deep vadose zone, NO_3^- concentrations are highest either in the topsoil (0-10 cm) or just below the root zone (~1-2 m) where NO_3^- is transported out of reach of roots with irrigation (Waterhouse et al., 2021, 2020). NO_3^- in soils can originate from N-based fertilizer or from N transformations, such as nitrification of ammonium (NH_4^+)-based fertilizer or nitrification of NH_4^+ from mineralized soil organic-N (Stein and Klotz, 2016). In contrast, NO_3^- removal pathways are denitrification and immobilization (controlled by microbial activity), leaching (controlled by infiltration rate), and plant uptake (Kurtzman et al., 2021; Long et al., 2013; Schmidt et al., 2011; Zhang et al., 2018). The governing processes during Ag-MAR are NO_3^- leaching, mineralization, nitrification, and denitrification (Murphy et al., 2021; Schmidt et al., 2012; Waterhouse et al., 2021). The latter is favored under suboxic to anoxic conditions, as expected during soil saturation of Ag-MAR events (Ganot and Dahlke, 2021b). N transformation processes, excluding leaching, occur in the soil dependent on electron donor availability (e.g., dissolved organic carbon (DOC)) and microbial community abundance and composition

(Peterson et al., 2013; Scarlett et al., 2021). Ambient conditions may also influence NO_3^- transformations, including soil moisture, carbon/nitrogen ratio, pH, soil texture, temperature, vegetation, oxidation-reduction potential (ORP), and water residence time in the topsoil (Kraft et al., 2014; Stein and Klotz, 2016). The underlying assumption adopted by previous researchers is that NO_3^--related processes are negligible below the root zone; therefore, NO_3^- leached below the root zone will eventually reach the groundwater (Baram et al., 2016b; Gurevich et al., 2021). Thus, in Ag-MAR, the aim is to reduce legacy NO_3^- via denitrification before NO_3^- leaching occurs below the root zone.

NO_3^- leaching is an environmental risk that is not unique to Ag-MAR, but can occur in any MAR method (e.g., infiltration basins; Beganskas et al., 2018), since it mainly depends on the source of NO_3^- in the recharge environment. For example, Beganskas et al. (2018), Gorski et al. (2019), and Schmidt et al. (2011) recharged stormwater runoff from upslope agricultural fields in an infiltration basin in the Pajaro Valley, California, which contained 22-25 mg L^{-1} NO_3^--N. If low-N source water is used in Ag-MAR (e.g., mountain runoff or snowmelt), elevated NO_3^- in soil pore water often originates from the soil matrix from recurring fertilizer applications.

Only a few studies exist to date that have estimated soil NO_3^- biogeochemical transformations and NO_3^- leaching under Ag-MAR. As one of the first, Bachand et al. (2014) investigated NO_3^- fate in a large farm-scale experiment where they flooded alfalfa, wine grapes, tomatoes, and fallow land for various periods ranging from 10 days to one month. They proposed a general framework for NO_3^- fate under Ag-MAR, concluding that NO_3^- will be leached to groundwater, but pore water and groundwater NO_3^- concentrations will be diluted following consecutive flood applications (assuming the use of low-NO_3^- water). However, they did not investigate any N transformations. Waterhouse et al. (2020) estimated the potential risk of NO_3^- leaching under Ag-MAR using only data from 10 m deep soil cores from 12 fields (no flooding was performed), focusing on three crops (almonds, processing tomatoes, and wine grapes) and two soil groups (low- and high-infiltrating soils). They concluded that vineyards were the most suitable crop for Ag-MAR due to low legacy NO_3^- resulting from the crop's deep roots and overall low N inputs.

Murphy et al. (2021) investigated the role of flooding frequency (i.e., three flooding events of 0.15 m depth each) and soil texture on N dynamics and potential NO_3^- leaching in laboratory column experiments. Each flooding event was on the scale of hours followed by a drying period of several days to two weeks. They observed that the majority of initially present soil NO_3^- leached during the first few hours of the first water application when conditions for denitrification (i.e., removal of NO_3^-) were unfavorable due to oxic conditions. NO_3^- leaching was quantified only for the laboratory column experiments ranging between 0.028 and 0.072 g NO_3^--N m^{-2} for every 1 cm^3 cm^{-2} of applied water. Based on the combination of lab assay and field data Murphy et al. (2021) showed that using only soil core data from pre- and post-flooding is insufficient to quantify NO_3^- leaching, emphasizing the need for continuous field measurements during Ag-MAR.

In a recent modeling study, Waterhouse et al. (2021) investigated Ag-MAR effects on denitrification rates and NO_3^- leaching in a heterogeneous, layered deep vadose zone (~15 m). They found that denitrification rates were highest in response to one continuous extensive water application due to the development of suboxic conditions compared to small incremental recharge events. However, this continuous water application scenario also leached NO_3^- deeper into the vadose zone. None of the above studies measured N-related biogeochemical processes during continuous, long (e.g., several weeks) flooding applications for Ag-MAR in different soils. This suggests that understanding of N fate and NO_3^- leaching at the field scale is still elusive in Ag-MAR; thus, further research is needed.

This study aims to investigate the environmental impacts of Ag-MAR using a large-scale field experiment conducted in the Central Valley, California (semiarid Mediterranean climate). Two vineyards, each with a different soil texture, were simultaneously flooded during late winter, one for four weeks (V1) and the other for two weeks (V2). Combining hydrologic, geochemical, and microbial process analyses, we quantified the effects of Ag-MAR on the soil N biogeochemical transformations, potential NO_3^- leaching to groundwater, soil physico-chemical conditions, and crop response. The results from this research, combined with data from previous studies, are summarized in a new conceptual model for integrated water-N dynamics.

2. Materials and Methods

2.1. Description of site, water application, and measurements

A replicated field experiment was conducted at the Kearney Agricultural Research and Extension Center (http://kare.ucanr.edu/) located 20 km southeast of the city of Fresno in the Central Valley of California, USA. Two mature (>40-year-old) own-rooted 'Thompson Seedless' grapevine (*Vitis vinifera* L.) vineyards were flooded; the first vineyard for four weeks (V1) and the second vineyard for two weeks (V2) (February–March 2020). V1 is on a very deep fine sandy loam (*Hesperia,* coarse-loamy, mixed, nonacid, thermic Xeric Torriorthents) with a saturated hydraulic conductivity (K_{sat}) of 0.02 m hr^{-1} for the first 1 m depth (USDA-NCSS soil survey data), and V2 is on a fine sandy loam (*Hanford*) with a K_{sat} of 0.1 m hr^{-1} for the first 1 m depth. Using a randomized complete block design, each vineyard was divided into six individual subplots, of which three were artificially flooded and three were kept under the natural precipitation regime (i.e., control) (**Fig. 1a**). Individual subplots were separated from one another using berms approximately 0.5 m high and 0.8 m wide (see **Fig. 1b**). The groundwater table was ~23 m below the surface measured in October 2019. The site has a semiarid, Mediterranean climate (Onsoy et al., 2005). Mean air temperature and total precipitation during the flooding period was 21.9 °C and 0.03 m, respectively.

Flooding started automatically at 06:00, 14:00, and 22:00 for 2-3 hrs at both vineyards each day, except for the first four days during which manual operation was used to adjust flow rates to prevent overflow to adjacent fields. Flooding of the vineyards started on 02/25/2020 and ended on 03/10/2020 (V2) and 03/24/2020 (V1). Two flow meters were used at the water inlet point of each vineyard to measure total applied water. Flooding was done using a single water outlet located at the west side of each row within the flooded subplots. A total of 7298 and 4659 m^3 were discharged at V1 and V2, respectively. Commonly Ag-MAR would be conducted using surface water. However, due to drought during the winter of 2019-2020 no surface water was available at our experimental site, therefore, pumped groundwater was used as an alternative water source for Ag-MAR. Groundwater was determined as a suitable alternative to surface water because N species concentrations in groundwater were found to be comparable to those of surface water in this area, as previously reported by Bachand et al. (2014).

Ten monitoring profiles were instrumented for continuous measurements, five within each vineyard (**Fig. 1a**). Out of the five profiles in each vineyard, only one profile was installed in the control (i.e., the non-flooded subplots) to allow higher spatial measurement resolution in the Ag-

MAR treatment subplots, which are the focus of this study. Each profile was installed 0.7 m from the vine row toward the furrow and included three sensor clusters at 0.2, 0.6 and 1 m depth. Each cluster included measurements of soil moisture and temperature (TEROS12, Meter, WA, USA), O_2 in gaseous phase (KE-25, Figaro, Japan), and ORP using constructed platinum electrodes (following Owens et al., 2005) and commercial Ag/AgCl reference electrodes (Accumet, Thermo Fisher Scientific, MA, USA). Additional measurements included three pressure transducers within stilling wells to record ponding levels (CS451, Campbell Scientific, UT, USA). Sensors were placed in hand augered holes that were backfilled with soil while compacting it at approximately 0.2 m intervals. Data were logged (CR1000 and CR800, Campbell Scientific, UT, USA) at a 10-min interval. The complete site and sensor descriptions are detailed in **Figs. 1a** and **1c**, respectively, and a photo taken during the flooding is presented in **Fig. 1b**. Atmospheric measurements (temperature, precipitation) at 60-min intervals were taken from the California Irrigation Management Information System station (CIMIS; station 39 Parlier, CA) situated 400 m from the experimental site.

Crop management practices followed standard recommendations with grape harvest in September and cane pruning on 20 January 2020. Both vineyards were fertilized once per year, two months after the flooding (end of April 2020), when 336 kg ha^{-1} of N fertilizer (ammonium sulfate 21-0-0 with 24% sulfur) were applied. Vines were manually harvested on 23 September 2020. The entire amount of fruit harvested from each plot was recorded and used for statistical analyses.

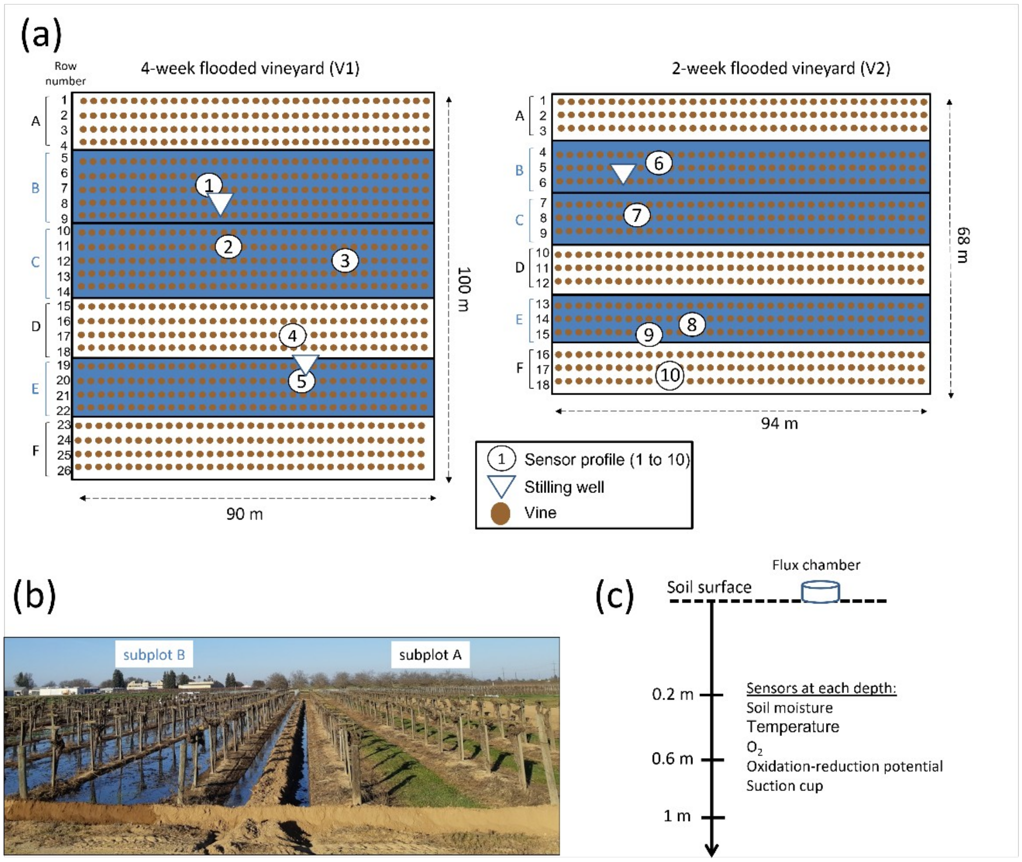

Fig. 1. Experimental setup. (a) Sensor locations in each vineyard. Flooded subplots are marked in blue. (b) A photo of the 4-week flooded vineyard (V1) showing subplots A and B during the flooding. (c) Sensor locations within a single profile.

2.2. *Pore water, gas emission, and soil sampling*

Pore water, greenhouse gas (GHG) emission, and soil sampling campaigns were carried out to better understand and quantify the N biogeochemical processes within the soil. Pore water samples were taken using suction cups (LT-DBL, Irrometer, CA, USA), installed at each of the ten profiles and at the same depths as the sensor clusters (0.2, 0.6, and 1 m). After installation, suction cup boreholes were backfilled with sieved soil slurry, followed by 0.15 m of soil, and sealed with 0.05 m bentonite; shallow 0.2 m suction cups were installed without bentonite. Pore water was sampled on average twice a week during the flooding period and once a week at other times, except for one continuous 5-day measurement campaign after fertilization to capture the fertilization effect on N processes. Samples were stored on ice until storage in a 4 °C cold room. Pore water was analyzed for NO_3^-, NH_4^+, and DOC. Analytical protocols are detailed in the supporting information.

In-situ GHG emissions were measured using the closed-flux vented chamber method (e.g., Garland et al., 2014). Twenty individual chambers were installed, each made from 0.26 m diameter polyvinyl chloride (PVC) pipe, consisting of a bottom ring and a cap. Two chambers were installed near each of the ten sensor profiles shown in **Fig. 1a** – one on the mount between the vines and one in the furrow. Collars were inserted into the soil to a depth of 0.07 m and left in the same location for the entire duration of the experiment. Chamber headspace was measured after each sampling to account for any reduction in volume due to water within the chamber. At sampling time, the chambers were sealed onto the collars with a rubber sleeve made from a tire innertube. Gas samples were taken through a rubber septum at four times (0, 30, 60, and 80 min) using a 20 mL air-tight syringe and injected into pre-evacuated 12 mL vials. Before each sampling effort, a 12V fan (installed within each chamber) was activated for 20-30 seconds to ensure a mixed representative headspace sample. Temperature was measured during each time step in 10 out of the 20 chambers. Samples were analyzed using a gas chromatograph (Shimadzu Trace Gas GC, Shimadzu Corp., Kyoto, Japan) for carbon dioxide (CO_2), methane (CH_4), and nitrous oxide (N_2O). Fluxes were calculated according to Garland et al. (2011). Gas samples were taken on similar days as the water samples and mostly around noon.

Soil samples were taken from four depths: 0-0.1, 0.1-0.2, 0.5-0.6, 0.8-1 m using a hand auger. All samples were taken from the same rows in which the sensor profiles were installed and at similar distances from the vines toward the furrow (~0.7 m). Samples were stored identical to pore water samples and taken during four campaigns according to the different experimental stages: 02/06/2020 (baseline data), 03/10/2020 (end of flooding at V2), 03/25/2020 (end of flooding at V1, and two weeks post-flooding at V2), and 04/15/2020 (three weeks post-flooding at V1). Soil samples were analyzed for NO_3^-, NH_4^+, DOC, and texture. In addition, soil subsamples were stored at -80 °C and later used for incubation experiments (see details in section 2.4).

2.3. Nitrogen leaching estimates

The amount of NO_3^- leaching below 1 m (the root zone in the case of flooded-irrigated vineyards) during flooding was quantified using a vadose-zone-based water and N mass balance model (Baram et al., 2016b), in which M_A is the cumulative mass of NO_3^- per flooded area (as NO_3^--N [g m^{-2}]) lost through leaching (**Eq. 1**) and M is the total mass of NO_3^- (as NO_3^--N [g]) lost during the flooding (**Eq. 2**):

$$M_A = \sum_{i=1}^{n} L_i C_i \Delta t_i \tag{1}$$

$$M = \sum_{i=1}^{n} M_{A_i} A \tag{2}$$

where L is the amount of water leaching below 1 m estimated using the infiltration rate (section 2.5) [m d^{-1}], C is the average NO_3^--N concentration in the leaching water at 1 m depth [g m^{-3}], Δt is a given time period [d] between each i^{th} measurement, and A is the flooded surface area [m^2].

Because all pore water NH_4^+ samples measurements at both vineyards were < 1 g m^{-3}, these values were considered negligible in the quantification of total inorganic N leached for modeling purposes.

2.4. Potential denitrification

Incubation experiments were conducted in the lab to assess denitrification rates during the flooding period. Net denitrification rates were estimated using a modified method of Petersen et al. (2012). Briefly, field-moist soil (15 g) collected one day before flooding and one day after flooding was added to 100 ml serum bottle and sealed with rubber stopper and metal caps, and then flushed with N_2 gas for 10 min to create anaerobic conditions and afterwards equilibrated with atmospheric pressure using a syringe. Bottles were placed in an incubator for 7 days at 25°C. Incubated samples were analyzed for changes in NO_3^- concentrations on the initial and 7th day to determine denitrification rates.

2.5. Hydrological analysis

Daily infiltration rates were calculated using two independent methods. In the first method, the total applied water was divided by the flooded surface area and total number of flooding days for each vineyard. The second method, also referred to as the falling head method, estimates the infiltration rate from the slope of the decreasing ponding level in each flood plot after water shut-off, which is then normalized for daily infiltration rates. Both methods provide bulk infiltration rates.

Groundwater recharge was calculated using a one-dimensional vertical water balance model (**Eq. 1**) (Dahlke et al., 2018). A single solution was solved for each of the eight flooded monitoring profiles using input data averaged over an hourly interval. The fraction of applied water going to deep percolation towards the groundwater table was calculated by accounting for evapotranspiration and storage in pore space.

$$R_t = I_t + P_t - ET_t - \Delta S_t - Q_t \tag{3}$$

where R_t [m] is recharge, I_t [m] is the amount of applied surface water, P_t [m] is precipitation, ET_t [m] is evapotranspiration, ΔS_t [m] is the change in soil storage, and Q_t [m] is surface runoff at time step t, which was assume to be negligible due to the use of berms. **Eq. 3** was solved using the Thornthwaite-Mather procedure (Steenhuis and Molen, 1986) performed via Excel solver (Office 365 ProPlus, 2020). This procedure was used in previous Ag-MAR studies (Dahlke et al. 2018). The procedure was solved for the first meter assuming this is also the maximum depth of the major root zone (Araujo et al., 1995) in which evapotranspiration demand takes place.

3. Results

3.1. Recharge and soil physical characteristics

The flood treatments in the two vineyards showed different hydrologic and biogeochemical responses during and after the flooding for recharge (V1 - **Fig. 2** and V2 – **Fig. 3**). As a result of field topography, flooding was not uniform in the flooded subplots. Dry areas occurred in the eastern part of V1 (**Fig. 1a**; subplot C) and V2 (**Fig. 1a**; subplots C and E), effectively reducing the flooded area to an average of 4613 m^2 (90%) and 3035 m^2 (75%) in V1 and V2, respectively. Soil ORP and O_2 concentration decreased rapidly in V1, reaching anoxic conditions (ORP < 100 Eh) at 0.2, 0.6 and 1 m depth 1-3 days after flooding started (**Figs. 2c** and **2d**). Reducing, anoxic conditions were sustained for 12-18 days after flooding ended, leading to ~40 days of continuous reducing conditions within the soil profile in V1. In contrast to V1, V2 maintained good aeration during the flooding and only experienced anoxic conditions at the shallowest depth of 0.2 m and for a short duration (2-5 days) (**Figs. 3c** and **3d**). O_2 and ORP averaged ~20% O_2 and ~400 Eh ORP at all other depths within the flooded soil profiles in V2. Although flooded plots at both vineyards reached near or fully saturated conditions as indicated by the soil moisture (**Figs. 2b** and **3b**), the observed differences in soil O_2 and ORP clearly indicate different environmental conditions that impacted biogeochemical processes in each vineyard.

As expected, control plots of both vineyards showed predominantly oxic ORP conditions (i.e., O_2 ~20% and ORP > 500 Eh) for the duration of the experiment and only abrupt soil moisture increases after rain events. The only exception was profile 4 in V1 (see **Fig. 1a** for location), which showed a soil moisture increase at 1 m depth followed by a decrease in O_2. Since no soil moisture increase was observed at 0.2 and 0.6 m, we attributed this change to the possibility of lateral flow from the flooded subplots, impacting the oxygen status in the deeper soil profile.

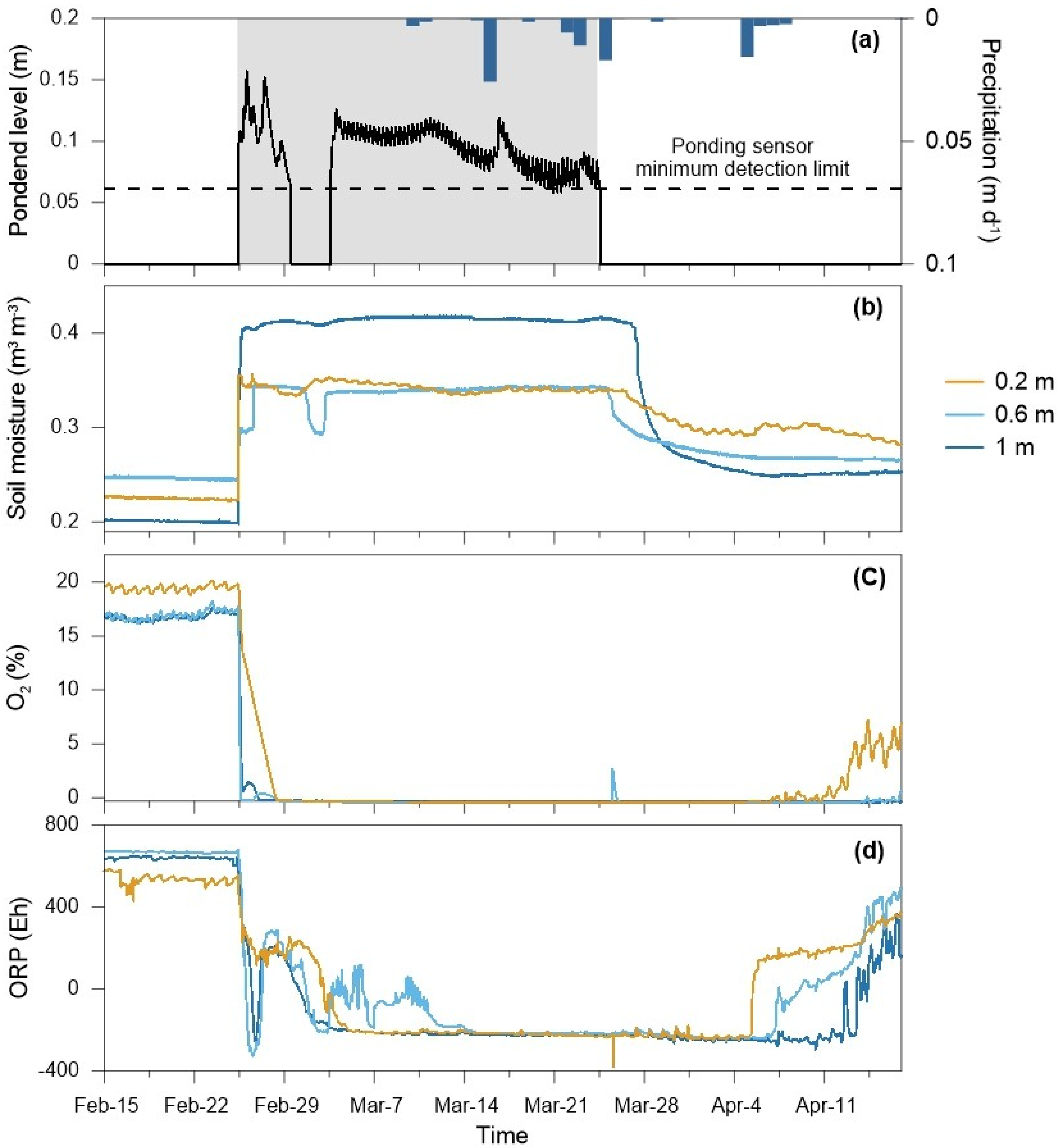

Fig. 2. Time series data for the 4-week flooded vineyard (V1) for selected hydrologic and physico-chemical parameters from profile 1 (see **Fig. 1a** for profiles location). ORP – oxidation-reduction potential. The gray shaded area in (a) shows the time of water application. Blue

precipitation bars show the daily totals taken from a meteorological station located 400 m from the experimental site.

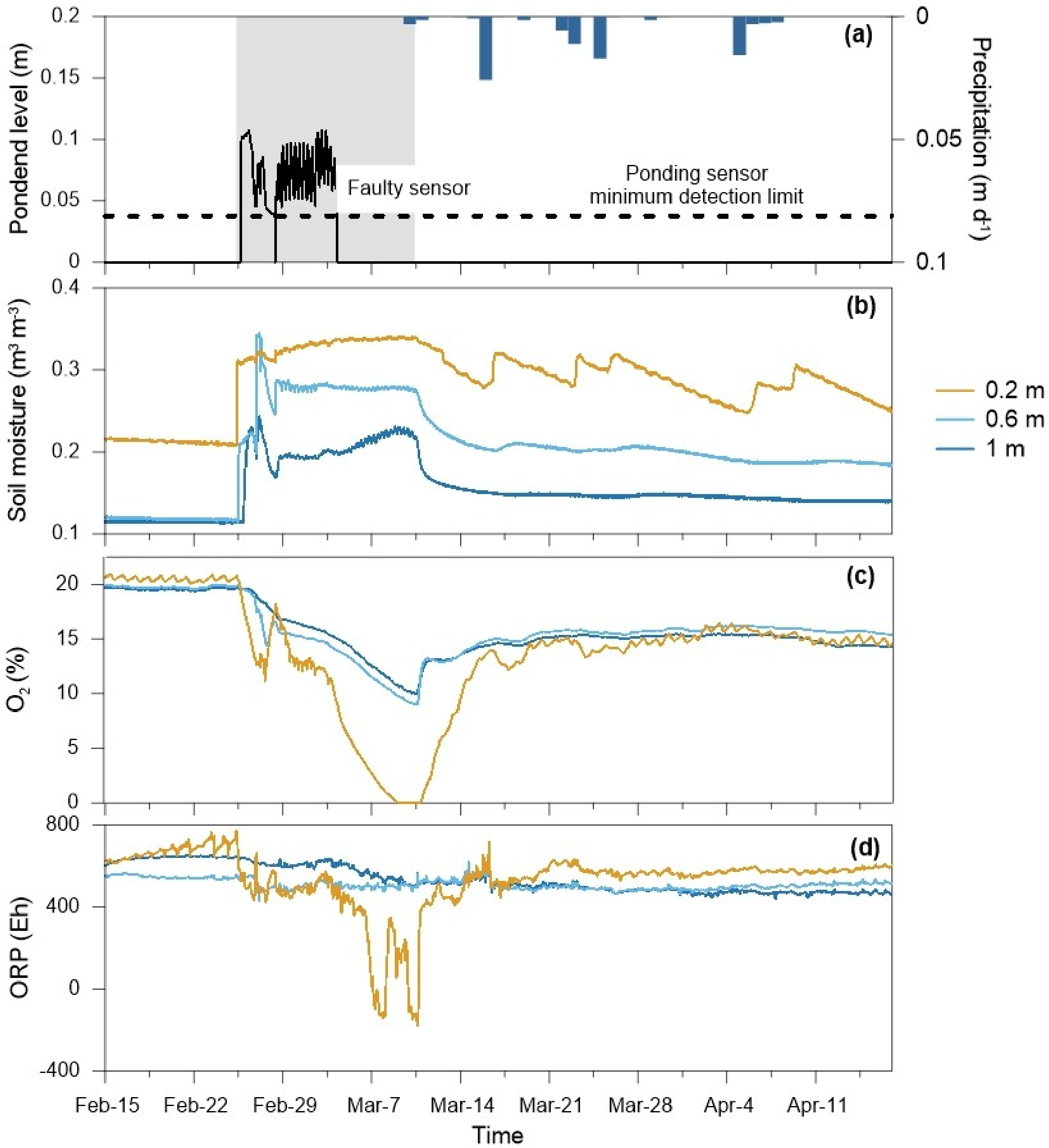

Fig. 3. Time series data for the 2-week flooded vineyard (V2) for selected hydrologic and physico-chemical parameters from profile 7 (see **Fig. 1a** for profiles location). ORP – oxidation-

reduction potential. Gray shaded area represents the flooding duration. Blue bars in plot a show daily precipitation totals.

3.2. *Infiltration rates and recharge*

The experimental site received little precipitation prior and during the experiment (**Fig. 2a**), thus providing an opportunity to study infiltration processes and water balance changes associated with Ag-MAR more closely. The infiltration rate in V1 was 0.088 ± 0.031 m d^{-1}. Estimated groundwater recharge was 83% ± 1.2% of the applied water using **Eq. 3**. The V2 site had a higher infiltration rate of 0.171 ± 0.025 m d^{-1} with 86% ± 0.7% of the applied water percolating below 1 m. The higher V2 recharge rate is also reflected by the soil suitability ranking developed by O'Geen et al. (2015) for California soils, which rates V2 as "excellent" for Ag-MAR whereas the ranking of V1 is "moderately good" as supported by soil textural analysis, which showed a higher sand fraction in V2 compared to V1 (**Fig. S1**). Upscaling the above values to each vineyard indicates that 1.31 and 1.32 m^3 m^{-2} of water was recharged in the flooded areas in V1 and V2, respectively. Although V2 was only flooded for two weeks, the higher infiltration rate (0.171 m d^{-1} in V2 compared to 0.088 m d^{-1} in V1) resulted in higher total recharge amounts.

3.3. *Pore water and residual soil chemistry*

Pore water NO_3^- and NH_4^+ data from both vineyards are presented in **Fig. 4**. During the first week of flooding, NO_3^- concentrations in both vineyards decreased to zero at all three depths (**Figs. 4b** and **4e**). Pore water NH_4^+ showed near-zero concentrations in the deeper soil profile (0.6 and 1 m) before flooding and a clear reduction at 0.2 m depth (**Figs. 4c** and **4f**). DOC concentrations in pore water remained approximately 20-60 mg DOC L^{-1} in both vineyards and at all depths during flooding (**Figs. 4a** and **4d**). Nitrite (NO_2^-) was not measured directly and assumed to be negligible following Bachand et al. (2014), which reported nitrite levels lower than 0.1 mg NO_2^--N L^{-1} during their Ag-MAR study.

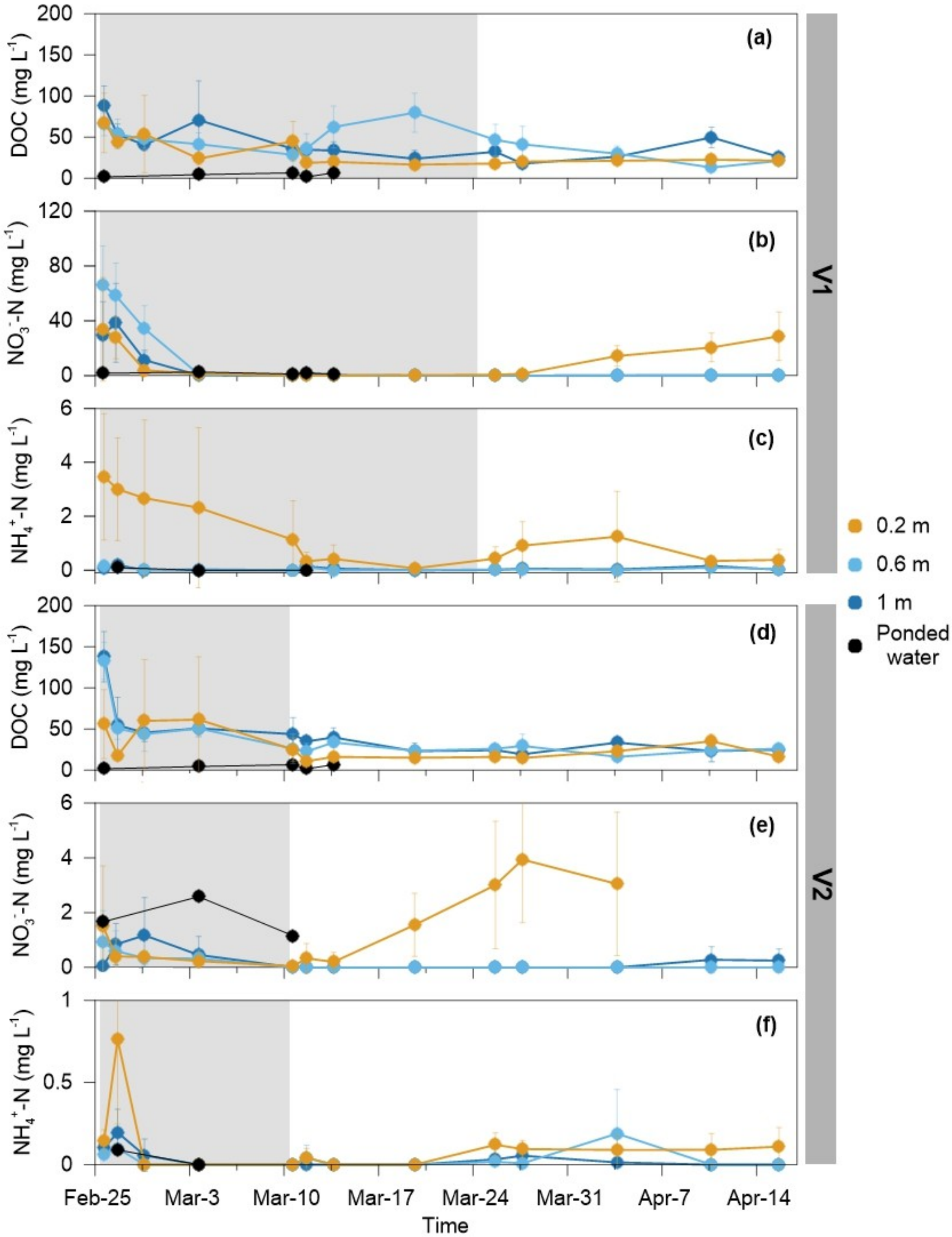

Fig. 4. Pore water results for the 4-week flooded vineyard (V1) (a-c) and the 2-week flooded vineyard (V2) (d-f). Values are averages of the four flooded profiles in each vineyard with error bars representing the standard deviation. Gray shaded areas represent the flooding duration.

Residual soil NH_4^+ in V1 depleted from 1-2 to near 0 mg NH_4^+-N kg^{-1} soil at all depths during the flooding (**Fig. 5a**). In V2, pre-flooding NH_4^+ concentrations were already low (e.g., ~0 mg NH_4^+-N kg $soil^{-1}$ below 0.1 m), with no significant change during flooding (**Figs. 5c** and **5d**). Two weeks after the flooding ended, NH_4^+ levels in both vineyards increased uniformly at all measured depths to ~1 and ~3 mg NH_4^+-N kg $soil^{-1}$ for V1 and V2, respectively (**Figs. 5a** and **5c**). Similar post-flooding trends of increasing concentrations were also observed for NO_3^- in both vineyards, however, only within the upper soil profile (0-0.2 m) where NO_3^- increased to 20-60 mg NO_3^--N kg^{-1} soil (**Figs. 5b** and **5d**).

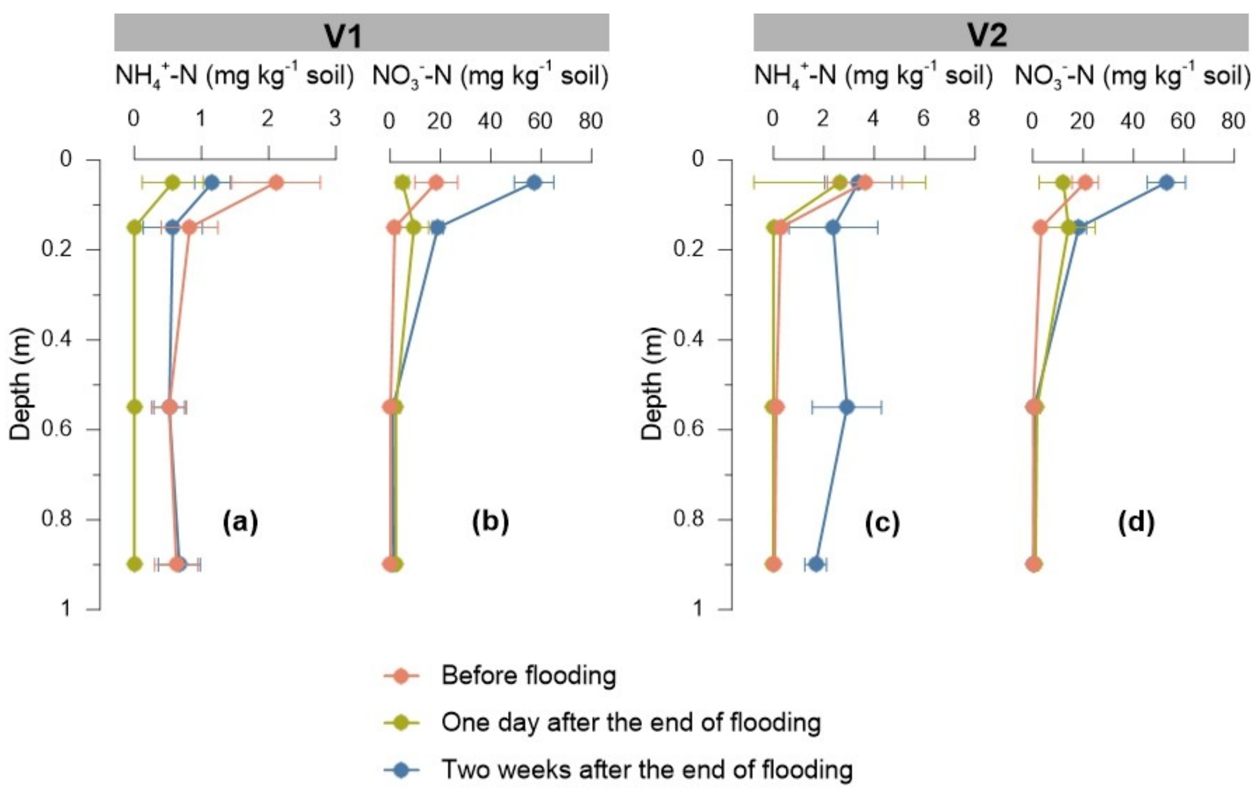

Fig. 5. Residual NO_3^- and NH_4^+ concentration in soil prior and after flooding for the 4-week flooded vineyard (V1) (a-b) and the 2-week flooded vineyard (V2) (c-d). Values are averages of the four flooded profiles in each vineyard with error bars representing the standard deviation.

3.4. Greenhouse gas emissions

During flooding, no changes in N_2O and CO_2 emissions were observed in the flood or control plots of V1 and V2 (**Fig. S2**). Post-flooding, N_2O emissions increased steadily for two weeks in the flooded plots in V1 before they declined again (**Fig. S2b**, blue line). However, peaks in N_2O and CO_2 emissions following the flooding were not as high as the spike observed two months after flooding, shortly after both vineyards received 336 kg ha^{-1} of N fertilizer (ammonium sulfate 21-0-0 with 24% sulfur; end of Apr-2020), which was the only fertilizer application during that year. We note that CH_4 emissions were not detected during the experiments.

3.5. Yield data

Both vineyards were harvested in early Sep 2020. In V1, a significant 29% decrease in yield was observed compared to the control (t-test, $p < 0.05$), whereas in V2, there was no evidence of a significant difference in yield although yield was 14% lower in the flooded plots ($p = 0.24$) (**Fig. S3**).

4. Discussion

4.1. Nitrate leaching vs. denitrification during flooding

We observed a rapid decline in pore water NO_3^- concentrations within the first days of flooding for Ag-MAR. Two possible processes can be attributed to the observed NO_3^- decrease: NO_3^-

removal due to denitrification, a microbial-controlled process, and/or leaching of NO_3^-, a solute transport process. The former would be preferable during Ag-MAR (or any other MAR type) since it can transform NO_3^- into the inert gas N_2, thereby preventing NO_3^- from reaching the groundwater (Levintal et al., 2022). Denitrification rates measured through incubation experiments (Petersen et al., 2012; Verchot et al., 2001), showed the highest denitrification activities in the top 0.1 m of the soil profile, decreasing to approximately zero below 0.6 m (**Fig. S4**). Denitrification rates in the top 0.1 m were 1.4 and 1.35 mg NO_3^--N kg soil^{-1} d^{-1} for V1 and V2, respectively. These rates are considered maximum rates, since they were obtained under optimal conditions (25 °C, O_2 ~ 0%, C substrate addition), favoring denitrification over nitrification. In both vineyards, oxic conditions dominated the root zone before flooding started and during imbibition. Thus, it is expected that denitrification rates were lower than the rates derived from the incubation experiments, at least until the root zone became fully suboxic/anoxic.

Infiltration rates not only determined the transition from oxic to suboxic conditions in each vineyard, but also the rate at which NO_3^- was transported below the active denitrification zone in the topsoil (i.e., 0-0.2 m). **Fig. 6** describes the tradeoff between the development of suboxic/anoxic conditions and the depletion of NO_3^- at 0.2 m. To allow comparison between the vineyards, NO_3^- concentrations in each vineyard were normalized to the initial concentrations observed in each vineyard prior to flooding. V1 reached suboxic conditions at 0.2 m (ORP < 400 Eh) after one day of flooding, compared to V2 which developed suboxic conditions only after 10 days. When the transition from oxic to suboxic conditions occurred in V1, more than 80% of the initial NO_3^- was still available at 0.2 m depth (**Fig. 6a,** blue squares). In contrast, by the time V2 reached suboxic conditions only ~10% of the initial NO_3^- was available for denitrification (**Fig. 6a,** red squares), indicating that 90% was leached.

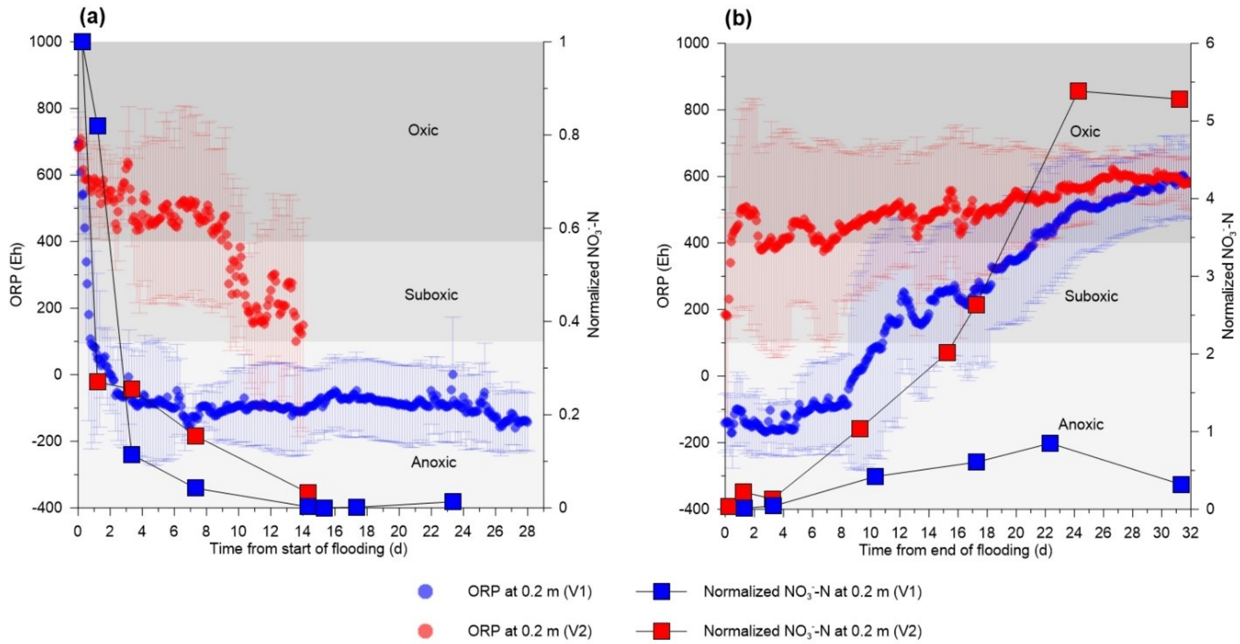

Fig. 6. Oxidation-reduction potential (ORP) and normalized pore water NO_3^- concentrations at 0.2 m depth during the wetting (a) and drying phase (b) of Ag-MAR. Values are averages of the flooded profiles in each vineyard with error bars representing the standard deviation. NO_3^- was normalized to the initial pore water NO_3^- concentrations in each vineyard; values above 1 indicate that NO_3^- exceeded the initial pre-flooding concentrations (i.e., V2 in subplot 'b').

The NO_3^- which was not consumed during the denitrification process in the topsoil was leached below the root zone and eventually transported towards the groundwater as denitrification is assumed to be negligible in the deep vadose zone (up to 3-5% per year) (Baram et al., 2016a). In both vineyards, the majority of NO_3^- was leached below 1 m during the first week of flooding, with a leaching peak of NO_3^- occurring during day 2 and 4 in V1 and V2, respectively (**Fig. 7a**). The cumulative amount of NO_3^- leached (using **Eqs. 1** and **2**) was 10.3 and 1.6 g NO_3^--N m^{-2} for

V1 and V2, respectively (**Fig. 7b**), which equates to a NO_3^- loading of 47.4 and 4.3 kg NO_3^--N for V1 (flooded area of 4,613 m^2) and V2 (flooded area of 3,035 m^2) below 1 m, respectively. Averaging the cumulative NO_3^- leached per total applied water results in 8.6 and 1 g NO_3^--N m^{-2} for every 1 cm^3 cm^{-2} of water applied for V1 and V2, respectively (i.e., an average leaching concentration of 8.6 and 1 mg L^{-1} NO_3^--N for V1 and V2). These values are similar in magnitude to NO_3^- leaching amounts estimated in a previous Ag-MAR field experiment (Bachand et al., 2014) and in an Ag-MAR column experiment (Murphy et al., 2021). Yet, it is also possible to have different leaching amounts between sites due to site-specific factors influencing nitrate leaching (e.g., soil texture and soil pre-flooding NO_3^- concentration).

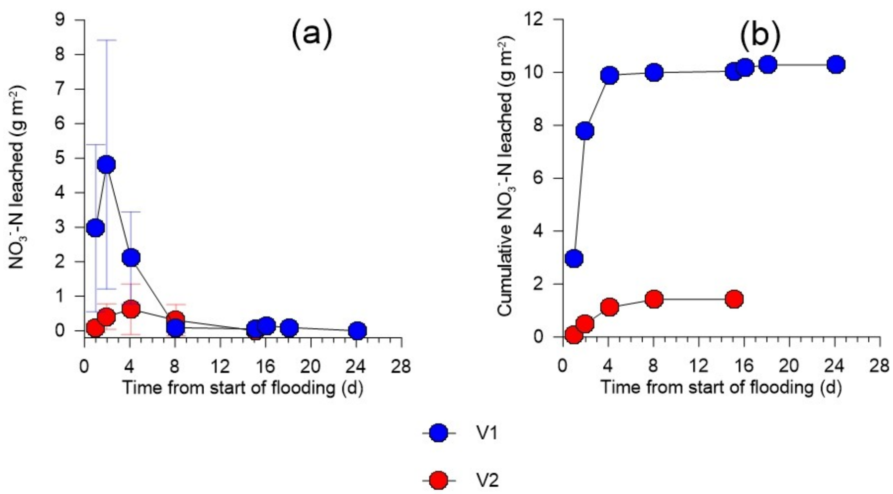

Fig. 7. Observed and cumulative amounts of NO_3^- leached below 1 m for (a) the 4-week flooded vineyard (V1) and (b) the 2-week flooded vineyard (V2).

The amount of NO_3^- leached differed by one-order of magnitude between the two vineyards. These differences can be attributed to the initial pore water and soil NO_3^- concentrations prior to flooding. In V1, the pre-flooding pore water NO_3^- concentrations ranged between 20-80 mg NO_3^--

N L^{-1} (**Fig. 4b**), whereas in V2, concentrations were below 2 mg NO_3^--N L^{-1} (**Fig. 4e**). Therefore, estimating legacy NO_3^- levels prior to Ag-MAR is essential for assessing leaching risks. It is emphasized that the low initial NO_3^- concentrations in V2's topsoil does not necessarily indicate a lower risk of groundwater contamination. Both vineyards were fertilized and irrigated following the same protocols in the years prior to the Ag-MAR experiment, and therefore, it is likely that elevated NO_3^- levels were also present in V2. Yet, the surplus NO_3^- was pushed deeper into the soil profile with each flood irrigation and precipitation event due to the higher infiltration rate of V2 compared to V1.

Once pre-flooding pore water NO_3^- depleted, concentrations in both vineyards and at all three measured depths (0.2, 0.6, and 1 m) stayed zero for the remainder of the flooding even though NO_3^- was added to the system with the floodwater (2-3 mg NO_3^--N L^{-1}; **Figs. 4b** and **e**, black circles). The source water NO_3^- was depleted by denitrification in the first 0.1 m of the soil profile. This conclusion is supported by the denitrification rates estimated through lab incubation experiments. For example, the denitrification rate estimated for the top 0.1 m soil profile in V1 was 1.4 mg NO_3^--N kg $soil^{-1}$ d^{-1} (**Fig. S4**), which translates to a potential *in-situ* soil denitrification of 10 mg NO_3^--N per day during flooding. This rate is ~5-fold higher than the floodwater NO_3^- concentration, thus can explain the NO_3^- depletion during infiltration. At this stage, water percolating below 1 m contributed to the dilution of the already leached residual soil NO_3^-. This process is also refereed as the dilution effect (Bachand et al., 2014). While Ag-MAR with low-contaminant water (e.g., rainfall-runoff or snowmelt) can cause not only NO_3^- leaching from the root zone, but also dilution of NO_3^- in pore water, its final impact on groundwater quality is a long-term process, which depends on several factors including the legacy NO_3^- load in the vadose zone, the NO_3^- concentration of groundwater, geogenic sources, and groundwater flow velocity (Dahan et al., 2014; Levintal et al. 2022). Therefore, quantifying the dilution effect from a single year is not feasible; further discussion is given below in section 4.3.

4.2. Post-flooding nitrogen dynamics

Owing to the legacy of N in agricultural plant systems, we investigated the post-flooding N cycling processes during the growing season. In V1, soil NH_4^+ levels recovered to pre-flooding levels in the first two weeks after the flooding ended (**Fig. 5a**). An increase was also observed for NO_3^-, however, only in the topsoil (**Fig. 5b**, 0-0.2 m). Similar post-flooding NH_4^+/NO_3^- concentrations increases were observed in V2 (**Figs. 5c** and **5d**), while NH_4^+ increased at all depths, NO_3^- increased only in the topsoil, indicating that mineralization occurred throughout the 1 m profile, whereas nitrification was mainly limited to the topsoil. NH_4^+ concentrations were an order-of magnitude lower than NO_3^- for both pore water and soil. The accumulation of NO_3^- in the top of the soil profile (0-0.2 m) rather than at deeper layers is consistent with previous studies (e.g., Dahan et al., 2014) who concluded that this accumulation pattern is preferable for both crop uptake and reducing leaching risks.

NO_3^- in pore water is considered to be more mobile in the vadose zone compared to the immobile NH_4^+ cations attached to soil particles and organic matter (Subbarao and Searchinger, 2021). In terms of NO_3^- leaching risk, the chemical composition of the pore water has a more immediate and significant effect on groundwater, rather than contaminants adsorbed onto sediment in the immobile phase. Thus, prioritization of pore water data over soil data is potentially recommended when assessing NO_3^- leaching risk to groundwater. We emphasize that additional research is needed to validate this statement as previous studies also suggested that nitrogen can be released from the soil to the pore water at later stages of the flooding and in the deep vadose zone (Mienis and Arye, 2018; Xin et al., 2019). In general, the relationship between pore water and soil samples is complex (Darrouzet-Nardi and Weintraub, 2014; Rimon et al., 2011). Studies suggested equations to convert between the two (Zhu et al., 2021). Yet, to date, no empirical relationship has been validated for different soils or soil moisture variations as expected during flooding.

Anoxic conditions continued in V1 for about 3 weeks after the flooding ended, while V2 stayed mostly in oxic conditions throughout and after the flooding (**Fig. 7b**). The topsoil (0.2 m) in V1's flooded area stayed in anoxic/suboxic conditions for 20 consecutive days once flooding ended, promoting denitrification. We observed elevated N_2O emissions, which can be a byproduct of denitrification, in the 20 days of anoxic/suboxic conditions following the flooding of V1 (**Fig. S2b**, blue circles during the start of April). We note that N_2O emissions can also be attributed to nitrification, however, under near-saturated conditions denitrification dominates N_2O production (Bateman and Baggs, 2005; Zhu et al., 2013). N_2O emissions started to decrease in V1 after the 20 days due to developing oxic conditions following flooding. N_2O emissions started to increase again after the vineyard's fertilization and first irrigation of the growing season on 4/29/2021. The measured N_2O emissions were similar in magnitude to reported fertilization-related emissions from vineyards under a similar Mediterranean climate (Garland et al., 2014, 2011).

4.3. Conceptual model – coupling nitrogen and water dynamics under Ag-MAR

We developed a conceptual model for N fate and transport in agricultural soils flooded for extended periods of time with low-contaminant water for Ag-MAR (**Fig. 8**). The model was developed based on data from the two vineyards investigated in this study and from recent Ag-

MAR studies conducted on alfalfa (Dahlke et al., 2018), almonds (Ganot and Dahlke, 2021b, 2021a), and in controlled soil column experiments (Murphy et al., 2021). We identify four stages that determine N fate during Ag-MAR: pre-flooding, start of flooding, quasi-steady flooding, and post-flooding. In each stage, the N fate is determined by the soil physico-chemical characteristics and the initial N concentration.

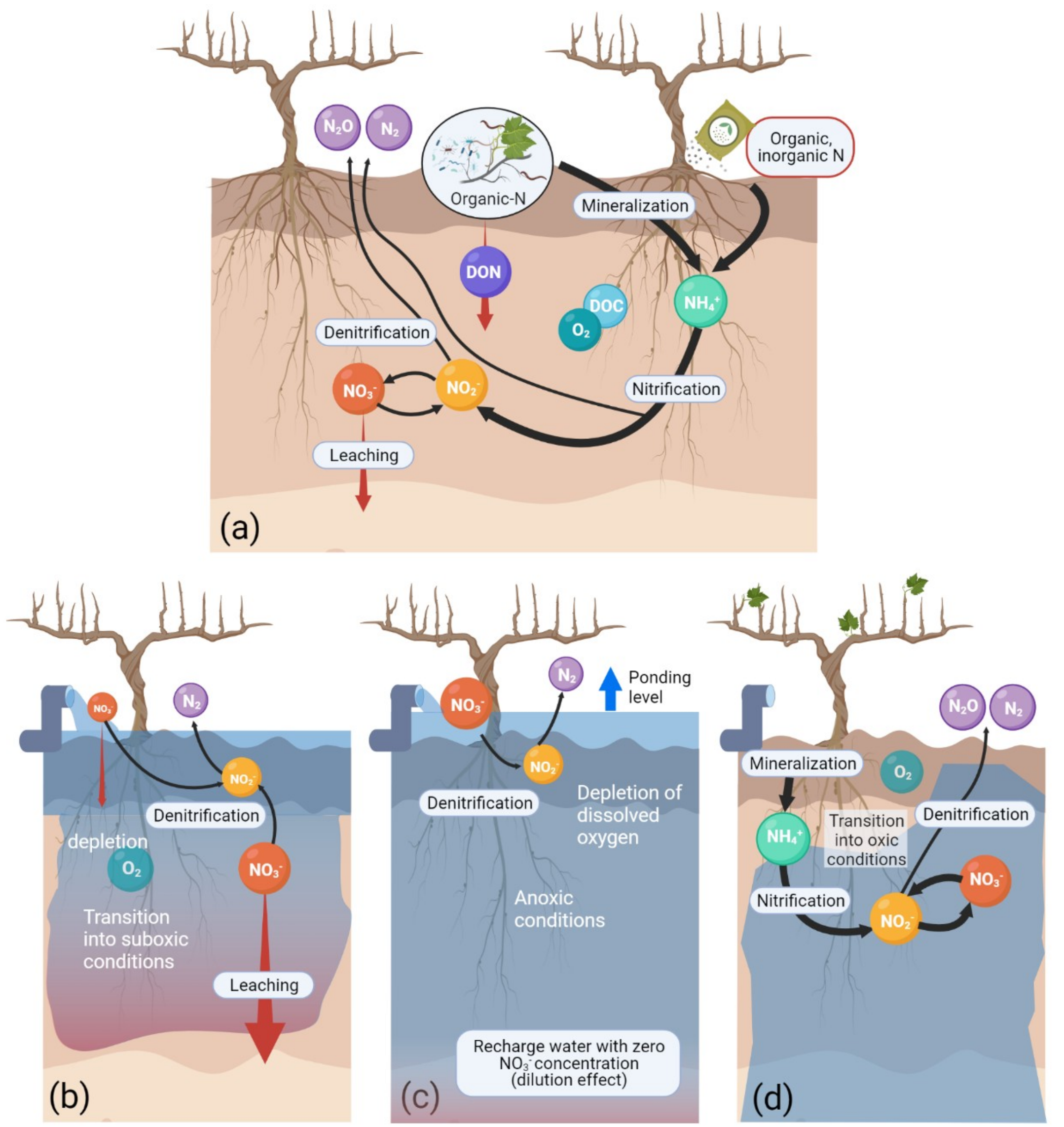

Fig. 8. Conceptual model for N fate under long-term flooding conditions at the topsoil. (a) pre-flooding, (b) start of flooding, (c) quasi-steady flooding, and (d) post-flooding. Detailed description for each stage is given in section 4.3. Figure created with Biorender.

Pre-flooding stage: In the pre-flooding stage (**Fig. 8a**), the root zone is unsaturated and predominantly oxic. The soil matrix and pore water contain variable amounts of legacy inorganic N species (i.e., NH_4^+ and NO_3^-) from previous fertilization events and from mineralization of organic-N, which are either transported with the infiltrating water or transformed through various microbial processes.

Start of flooding stage: With the start of flooding (**Fig. 8b**) the root zone saturates with water thereby decreasing oxygen and ORP levels. This is the most dynamic stage during the flooding event, yet with high environmental significance as this stage will define the magnitude of the NO_3^- leached. The amount of NO_3^- leached below the root zone and the amount of NO_3^- denitrified in the topsoil is dependent on site-specific physico-chemical parameters (K_{sat}, infiltration rate, ORP, available NO_3^- and carbon, and temperature) and the abundance and activity of both nitrifying and denitrifying microbial communities in the topsoil. NO_3^- leaching is the dominating loss process in soils with high K_{sat} (or infiltration rate), while denitrification plays a larger role in soils with lower K_{sat} where the residence time of water in the topsoil is longer. Of course, denitrification is the preferred loss pathway for NO_3^- to reduce NO_3^- contamination to groundwater, however, in the time it takes to reach suboxic conditions that promote denitrification, high K_{sat} soil might already leach > 80% of the legacy NO_3^- present in the profile.

Quasi-steady flooding stage: After the highly dynamic NO_3^- leaching and N transformation phase at the start of flooding, the system transitions into the quasi-steady flooding stage (**Fig. 8c**), which is characterized by saturated, suboxic/anoxic conditions and more stable soil physico-chemical parameters. If anoxic conditions are reached in the root zone, it can be assumed that dissolved oxygen is likewise depleted as reported in other MAR studies (Turkeltaub et al., 2022). Under these conditions, denitrifiers in the topsoil consume NO_3^- in the infiltrating water. This NO_3^- removal will eventually contribute to the dilution of pore water NO_3^- in the vadose zone. Sustaining the quasi-steady flooding stage for as long as possible is preferred because it increases the amount of 'clean' recharge while reducing NO_3^- levels in the pore water transported to groundwater. However, the dilution effect only takes effect if NO_3^- concentrations in the source water are relatively low and the retention time of the infiltrating water in the denitrifying soil layer is sufficiently long to allow complete NO_3^- consumption. For example, in this study, infiltration rates of 0.1-0.2 m d^{-1} were sufficient to allow denitrification of NO_3^- in the source water (2-3 mg NO_3^--N L^{-1}) in the first 0.2 m of the soil profile. If recharge water is sourced from pristine streamflow, it is typically low in NO_3^- concentrations. Hence, there is a high probability for the dilution effect to occur during the quasi-steady flooding stage when implementing Ag-MAR for periods of more than several days. However, flooding fields for long periods of time might negatively impact crop performance, as shown for V1, which needs to be considered and balanced (Levintal et al., 2022). A possible solution is to use a new model that predicts crop damage as a function of the duration of saturated conditions in the soil root-zone, soil texture, and crop tolerance to waterlogged conditions (Ganot and Dahlke, 2021a).

Post-flooding stage: In the post-flooding stage (**Fig. 8d**), oxygen and ORP will gradually increase back to pre-flooding oxic levels. In soils with higher infiltration rates (sand or loamy-sand) this process can take several days compared to several weeks in soils with lower infiltration rates (e.g., sandy loam or loam). Soil moisture will also decrease from near- or full-saturation to pre-flooding levels. However, this process is relatively slow (on the scale of weeks to months) and controlled also by precipitation or irrigation events that will temporarily increase soil moisture in the root zone. A post-flooding increase in NO_3^- and NH_4^+ is also expected, mainly in the topsoil (0-0.2 m) as a result of mineralization and nitrification. Denitrification is another post-flooding process that can occur, yet it will be more pronounced in soils with slow infiltration rates when soil moisture is still high during the first stage of drainage when anoxic/suboxic conditions prevail (V1 in this study).

Ag-MAR includes three distinct differences compared to other MAR types (Goren et al., 2014; Gorski et al., 2020, 2019; Mienis and Arye, 2018): (1) the nitrogen source is mainly in the soil rather than in the recharge water, (2) recharge (i.e., the flooding) will be primarily seasonal during wet periods and not yearly with continuous flooding and drying cycles, and (3) the infiltration basin is not necessarily on high-infiltrating land, such as sandy soil. Therefore, caution should be taken when adapting the four model's stages for long-term flooding of other MAR types. For example, nitrogen fate under soil aquifer treatment (SAT; a MAR form where treated wastewater is recharged) showed highly complex biogeochemical processes due to changing nitrogen and carbon loading (e.g. NH_4^+) in the source water (Mienis and Arye, 2018). This resulted in varying nitrate concentrations in the groundwater during the recharge, which our model cannot adequately explain.

4.4. Implications for Ag-MAR operation

Understanding the N-related dynamics at each stage of Ag-MAR as presented in the conceptual model (**Fig. 8**) is essential for the development of best management practices. Taking V1 as a case study, a better practice to decrease the risk of NO_3^- leaching would be to irrigate the vineyard initially for 1-2 days (before the continuous flooding for Ag-MAR) until anoxic conditions are developed, which would promote denitrification and minimize NO_3^- leaching. Maintaining anoxic conditions is also important for the inhibition of the nitrification process that can increase inorganic NO_3^- concentrations between individual recharge (i.e., flooding) events. The predicted outcome of the suggested recharge practice will be a decrease in the overall amount of NO_3^- leached. However, this practice is unlikely to be applicable in high infiltrating soils in which nearly all the initial NO_3^- will be leached in the first few days before the development of anoxic conditions (V2 in this study, infiltration rate of 0.171 m d^{-1}). A more detailed discussion on the trade-offs between leaching and mineralization–denitrification processes under repeated flooding events is provided by Murphy et al. (2021).

Our study was conducted in a Mediterranean climate, and therefore, adjustments are needed if adapting the findings to other locations. For instance, lower ambient soil temperatures will decrease the rate at which nitrification/denitrification occurs and to a lesser extent also influence the infiltration rate (Grinshpan et al., 2022). Thus, Ag-MAR implementation in colder climates will decrease denitrification rates during infiltration, potentially increasing the risk for leaching of soil residual NO_3^-. Other considerations for Ag-MAR implementation are non-point source contaminants with high leaching risks, such as salts, pesticides, and inorganic geogenic contaminates. A comprehensive review of these contaminants with potential solutions is provided in Levintal et al. (2022). Still, high NO_3^- concentration in the aquifer is the main concern at global scale (Beganskas et al., 2018; Dahan et al., 2014). With respect to yield, several reasons can explain the yield difference between the vineyards investigated in this study, such as differences in soil texture and the resulting K_{sat}, infiltration rates, O_2/redox levels, duration of flooding, movement of available N below root zone, and timing of flooding with respect to bud break in March. Therefore, possible effects on yield should be investigated in more detail, and until then, caution is advised in using Ag-MAR in late winter-early spring, in vineyards with less-than-ideal soil properties.

5. Conclusions

An agricultural managed aquifer recharge (Ag-MAR) experiment was conducted in the Central Valley of California on two vineyards managed similarly but differing in soil texture and hydraulic properties. One vineyard was flooded for four weeks (V1) and the other for two weeks (V2). Although the flooding for groundwater recharge started on the same day, different soil biogeochemical outcomes occurred. Suboxic conditions, favoring denitrification in the microbially active topsoil (0-0.2 m), developed in the vineyard with the low-infiltration rate (0.088 m d^{-1}; V1) in less than one day, compared to 10 days in the high-infiltration vineyard (0.171 m d^{-1}; V2). Nevertheless, in both vineyards, NO_3^- leaching was the dominant N loss process while denitrification played a lesser role in decreasing NO_3^- in the root zone. The amount of NO_3^- leached below the 1 m root zone was mainly determined by the amount of residual NO_3^- present in the root zone prior to the flooding for groundwater recharge, showcasing the importance of estimating legacy NO_3^- pools before establishing an Ag-MAR site.

A conceptual model for water-N dynamics under Ag-MAR was developed based on hydrologic, geochemical, and microbial process analyses. Four stages were identified: pre-flooding, start of flooding, quasi-steady flooding, and post-flooding. Out of the above, the start of flooding is the most dynamic stage that will define the magnitude of NO_3^- leached. The proposed model can be used to determine best Ag-MAR management practices. Adoption of Ag-MAR, as one approach in a portfolio of MAR methods, is desirable as population growth and expansion of irrigated agriculture contribute to unsustainable groundwater extraction and a growing need to replenish groundwater resources to buffer growing water supply variability.

CRediT authorship contribution statement

Elad Levintal: Methodology, Writing – original draft, Formal analysis. **Laibin Huang:** Writing - review& editing, Formal analysis. **Cristina Prieto García:** Methodology, Writing - review& editing, Formal analysis. **Adolfo Coyotl:** Writing - review& editing, Formal analysis. **Matthew W. Fidelibus:** Writing - review& editing, Formal analysis. **William R. Horwath:** Writing - review& editing, Funding acquisition. **Jorge L. Mazza Rodrigues:** Writing - review& editing, Funding acquisition. **Helen E. Dahlke:** Supervision, Methodology, Writing - review& editing, Funding acquisition.

Declaration of competing interest

The authors declare that they have no known competing financial interests or personal relationships that could have appeared to influence the work reported in this paper.

Acknowledgments

This research has been supported by the Gordon and Betty Moore Foundation (grant no. 7975) and the United States–Israel Binational Agricultural Research and Development Fund (Vaadia-BARD Postdoctoral Fellowship award no. FI-605-2020), the National Institute of Food and Agriculture (grant no. CA-D-LAW-2513-H), the California Department of Pesticide Regulation (contract no. 17-C0099), and USDA Natural Resources Conservation Agreement NR183A750023C005.

References

Araujo, F., Williams, L.E., Grimes, D.W., Matthews, M.A., 1995. A comparative study of young "Thompson Seedless" grapevines under drip and furrow irrigation. I. Root and soil water distributions. Sci. Hortic. (Amsterdam). 60, 235–249.

Bachand, P.A.M., Roy, S.B., Choperena, J., Cameron, D., Horwath, W.R., 2014. Implications of using on-farm flood flow capture to recharge groundwater and mitigate flood risks along the Kings River, CA. Environ. Sci. Technol. 48, 13601–13609.

Baram, S., Couvreur, V., Harter, T., Read, M., Brown, P.H., Hopmans, J.W., Smart, D.R., 2016a. Assessment of orchard N losses to groundwater with a vadose zone monitoring network. Agric. Water Manag. 172, 83–95.

Baram, S., Couvreur, V., Harter, T., Read, M., Brown, P.H., Kandelous, M., Smart, D.R., Hopmans, J.W., 2016b. Estimating nitrate leaching to groundwater from orchards: Comparing crop nitrogen excess, deep vadose zone sata-sriven estimates, and HYDRUS modeling. Vadose Zo. J. 15, 1–13.

Bateman, E.J., Baggs, E.M., 2005. Contributions of nitrification and denitrification to N2O emissions from soils at different water-filled pore space. Biol. Fertil. Soils 41, 379–388.

Beganskas, S., Gorski, G., Weathers, T., Fisher, A.T., Schmidt, C., Saltikov, C., Redford, K., Stoneburner, B., Harmon, R., Weir, W., 2018. A horizontal permeable reactive barrier stimulates nitrate removal and shifts microbial ecology during rapid infiltration for managed recharge. Water Res. 144, 274–284.

Bishayee, B., Chatterjee, R.P., Ruj, B., Chakrabortty, S., Nayak, J., 2022. Strategic management of nitrate pollution from contaminated water using viable adsorbents: An economic assessment-based review with possible policy suggestions. J. Environ. Manage. 303, 114081.

Connor, R., 2015. The United Nations world water development report 2015: Water for a sustainable world. UNESCO publishing, Paris.

Dahan, O., Babad, A., Lazarovitch, N., Russak, E.E., Kurtzman, D., 2014. Nitrate leaching from intensive organic farms to groundwater. Hydrol. Earth Syst. Sci. 18, 333–341.

Dahlke, H.E., Brown, A.G., Orloff, S., Putnam, D., O‘Geen, T., 2018. Managed winter flooding of alfalfa recharges groundwater with minimal crop damage. Calif. Agric. 72, 65–75.

Darrouzet-Nardi, A., Weintraub, M.N., 2014. Evidence for spatially inaccessible labile N from a comparison of soil core extractions and soil pore water lysimetry. Soil Biol. Biochem. 73, 22–32.

Dillon, P., Stuyfzand, P., Grischek, T., Lluria, M., Pyne, R.D.G., Jain, R.C., Bear, J., Schwarz, J., Wang, W., Fernandez, E., Stefan, C., Pettenati, M., van der Gun, J., Sprenger, C., Massmann, G., Scanlon, B.R., Xanke, J., Jokela, P., Zheng, Y., Rossetto, R., Shamrukh, M., Pavelic, P., Murray, E., Ross, A., Bonilla Valverde, J.P., Palma Nava, A., Ansems, N., Posavec, K., Ha, K., Martin, R., Sapiano, M., 2019. Sixty years of global progress in managed aquifer recharge. Hydrogeol. J. 27, 1–30.

Ganot, Y., Dahlke, H.E., 2021a. A model for estimating Ag-MAR flooding duration based on crop tolerance, root depth, and soil texture data. Agric. Water Manag. 255, 107031.

Ganot, Y., Dahlke, H.E., 2021b. Natural and forced soil aeration during agricultural managed aquifer recharge. Vadose Zo. J. 20, 1–19.

Garland, G.M., Suddick, E., Burger, M., Horwath, W.R., Six, J., 2014. Direct N2O emissions from a Mediterranean vineyard: Event-related baseline measurements. Agric. Ecosyst. Environ. 195, 44–52.

Garland, G.M., Suddick, E., Burger, M., Horwath, W.R., Six, J., 2011. Direct N2O emissions following transition from conventional till to no-till in a cover cropped Mediterranean vineyard (Vitis vinifera). Agric. Ecosyst. Environ. 141, 234–239.

Gorelick, S.M., Zheng, C., 2015. Global change and the groundwater management challenge. Water Resour. Res. 51, 3031–3051.

Goren, O., Burg, A., Gavrieli, I., Negev, I., Guttman, J., Kraitzer, T., Kloppmann, W., Lazar, B., 2014. Biogeochemical processes in infiltration basins and their impact on the recharging effluent, the soil aquifer treatment (SAT) system of the Shafdan plant, Israel. Appl. Geochemistry 48, 58–69.

Gorski, G., Dailey, H., Fisher, A.T., Schrad, N., Saltikov, C., 2020. Denitrification during infiltration for managed aquifer recharge: Infiltration rate controls and microbial response. Sci. Total Environ. 727.

Gorski, G., Fisher, A.T., Beganskas, S., Weir, W.B., Redford, K., Schmidt, C., Saltikov, C., 2019. Field and laboratory studies linking hydrologic, geochemical, and microbiological processes and enhanced denitrification during infiltration for managed recharge. Environ. Sci. Technol. 53, 9491–9501.

Grinshpan, M., Furman, A., Dahlke, H.E., Raveh, E., Weisbrod, N., 2021. From managed aquifer recharge to soil aquifer treatment on agricultural soils: concepts and challenges. Agric. Water Manag. 255, 106991.

Grinshpan, M., Turkeltaub, T., Furman, A., Raveh, E., Weisbrod, N., 2022. On the use of orchards to support soil aquifer treatment systems. Agric. Water Manag. 260, 107315.

Gurevich, H., Baram, S., Harter, T., 2021. Measuring nitrate leaching across the critical zone at the field to farm scale. Vadose Zo. J. 1–16.

Haddeland, I., Heinke, J., Biemans, H., Eisner, S., Flörke, M., Hanasaki, N., Konzmann, M., Ludwig, F., Masaki, Y., Schewe, J., Stacke, T., Tessler, Z.D., Wada, Y., Wisser, D., 2014. Global water resources affected by human interventions and climate change. Proc. Natl. Acad. Sci. U. S. A. 111, 3251–3256.

Kocis, T.N., Dahlke, H.E., 2017. Availability of high-magnitude streamflow for groundwater banking in the Central Valley, California. Environ. Res. Lett. 12.

Kraft, B., Tegetmeyer, H.E., Sharma, R., Klotz, M.G., Ferdelman, T.G., Hettich, R.L., Geelhoed, J.S., Strous, M., 2014. The environmental controls that govern the end product of bacterial nitrate respiration. Science (80-.). 345, 676–679.

Kurtzman, D., Kanner, B., Levy, Y., Nitsan, I., Bar-Tal, A., 2021. Maintaining intensive agriculture overlying aquifers using the threshold nitrate root-uptake phenomenon. J.

Environ. Qual. 1–11.

Levintal, E., Kniffin, M.L., Ganot, Y., Marwaha, N., Murphy, N.P., Dahlke, H.E., 2022. Agricultural managed aquifer recharge (Ag-MAR)—a method for sustainable groundwater management: A review. Crit. Rev. Environ. Sci. Technol. 0, 1–24.

Long, A., Heitman, J., Tobias, C., Philips, R., Song, B., 2013. Co-occurring anammox, denitrification, and codenitrification in agricultural soils. Appl. Environ. Microbiol. 79, 168–176.

Mienis, O., Arye, G., 2018. Long-term nitrogen behavior under treated wastewater infiltration basins in a soil-aquifer treatment (SAT) system. Water Res. 134, 192–199.

Murphy, N.P., Waterhouse, H., Dahlke, H.E., 2021. Influence of agricultural managed aquifer recharge on nitrate transport: The role of soil texture and flooding frequency. Vadose Zo. J. 20, 1–16.

Negri, C., Chiaradia, E., Rienzner, M., Mayer, A., Gandolfi, C., Romani, M., Facchi, A., 2020. On the effects of winter flooding on the hydrological balance of rice areas in northern Italy. J. Hydrol. 590, 125401.

Niswonger, R.G., Morway, E.D., Triana, E., Huntington, J.L., 2017. Managed aquifer recharge through off-season irrigation in agricultural regions. Water Resour. Res. 53, 6970–6992.

O'Geen, A.T., Saal, M., Dahlke, H., Doll, D., Elkins, R., Fulton, A., Fogg, G., Harter, T., Hopmans, J.W., Ingels, C., Niederholzer, F., Solis, S.S., Verdegaal, P., Walkinshaw, M., 2015. Soil suitability index identifies potential areas for groundwater banking on agricultural lands. Calif. Agric. 69, 75–84.

Onsoy, Y.S., Harter, T., Ginn, T.R., Horwath, W.R., 2005. Spatial Variability and Transport of Nitrate in a Deep Alluvial Vadose Zone. Vadose Zo. J. 4, 41–54.

Owens, P.R., Wilding, L.P., Lee, L.M., Herbert, B.E., 2005. Evaluation of platinum electrodes and three electrode potential standards to determine electrode quality. Soil Sci. Soc. Am. J. 69, 1541–1550.

Petersen, D.G., Blazewicz, S.J., Firestone, M., Herman, D.J., Turetsky, M., Waldrop, M., 2012. Abundance of microbial genes associated with nitrogen cycling as indices of biogeochemical process rates across a vegetation gradient in Alaska. Environ. Microbiol. 14, 993–1008.

Peterson, M.E., Curtin, D., Thomas, S., Clough, T.J., Meenken, E.D., 2013. Denitrification in vadose zone material amended with dissolved organic matter from topsoil and subsoil. Soil Biol. Biochem. 61, 96–104.

Richa, A., Touil, S., Fizir, M., 2022. Recent advances in the source identification and remediation techniques of nitrate contaminated groundwater: A review. J. Environ. Manage. 316, 115265.

Rimon, Y., Nativ, R., Dahan, O., 2011. Physical and Chemical Evidence for Pore-Scale Dual-Domain Flow in the Vadose Zone. Vadose Zo. J. 10, 322–331.

Scarlett, K., Denman, S., Clark, D.R., Forster, J., Vanguelova, E., Brown, N., Whitby, C., 2021. Relationships between nitrogen cycling microbial community abundance and composition reveal the indirect effect of soil pH on oak decline. ISME J. 15, 623–635.

Schmidt, C.M., Fisher, A.T., Racz, A., Wheat, C.G., Los Huertos, M., Lockwood, B., 2012. Rapid nutrient load reduction during infiltration of managed aquifer recharge in an agricultural groundwater basin: Pajaro Valley, California. Hydrol. Process. 26, 2235–2247.

Schmidt, C.M., Fisher, A.T., Racz, A.J., Lockwood, B.S., Huertos, M.L., 2011. Linking denitrification and infiltration rates during managed groundwater recharge. Environ. Sci. Technol. 45, 9634–9640.

Siebert, S., Burke, J., Faures, J.M., Frenken, K., Hoogeveen, J., Döll, P., Portmann, F.T., 2010. Groundwater use for irrigation - A global inventory. Hydrol. Earth Syst. Sci. 14, 1863–1880.

Steenhuis, T., Molen, W., 1986. The TM procedure as a simple engineering method to predict recharge. J. Hydrol. 84, 221–229.

Stein, L.Y., Klotz, M.G., 2016. The nitrogen cycle. Curr. Biol. 26, R94–R98.

Subbarao, G. V., Searchinger, T.D., 2021. A “more ammonium solution” to mitigate nitrogen pollution and boost crop yields. Proc. Natl. Acad. Sci. U. S. A. 118, 1–5.

Turkeltaub, T., Furman, A., Mannheim, R., Weisbrod, N., 2022. Continuous monitoring of a soil aquifer treatment system’s physico-chemical conditions to optimize operational performance. Hydrol. Earth Syst. Sci. 26, 1565–1578.

Van Meter, K.J., Basu, N.B., Veenstra, J.J., Burras, C.L., 2016. The nitrogen legacy: Emerging evidence of nitrogen accumulation in anthropogenic landscapes. Environ. Res. Lett. 11.

Verchot, L. V., Holmes, Z., Mulon, L., Groffman, P.M., Lovett, G.M., 2001. Gross vs net rates of N mineralization and nitrification as indicators of functional differences between forest types. Soil Biol. Biochem. 33, 1889–1901.

Wada, Y., Van Beek, L.P.H., Van Kempen, C.M., Reckman, J.W.T.M., Vasak, S., Bierkens, M.F.P., 2010. Global depletion of groundwater resources. Geophys. Res. Lett. 37, 1–5.

Waterhouse, H., Arora, B., Spycher, N.F., Nico, P.S., Ulrich, C., Dahlke, H.E., Horwath, W.R., 2021. Influence of Agricultural Managed Aquifer Recharge (AgMAR) and Stratigraphic Heterogeneities on Nitrate Reduction in the Deep Subsurface. Water Resour. Res. 57, 1–22.

Waterhouse, H., Bachand, S., Mountjoy, D., Choperena, J., Bachand, P.A.M., Dahlke, H.E., Horwath, W.R., 2020. Agricultural managed aquifer recharge - water quality factors to consider. Calif. Agric. 74, 144–154.

Weitzman, J.N., Brooks, J.R., Compton, J.E., Faulkner, B.R., Mayer, P.M., Peachey, R.E., Rugh, W.D., Coulombe, R.A., Hatteberg, B., Hutchins, S.R., 2022. Deep soil nitrogen storage slows nitrate leaching through the vadose zone. Agric. Ecosyst. Environ. 332, 107949.

Xin, J., Liu, Y., Chen, F., Duan, Y., Wei, G., Zheng, X., Li, M., 2019. The missing nitrogen pieces: A critical review on the distribution, transformation, and budget of nitrogen in the vadose zone-groundwater system. Water Res. 165, 114977.

Zhang, Y., Ding, H., Zheng, X., Cai, Z., Misselbrook, T., Carswell, A., Müller, C., Zhang, J., 2018. Soil N transformation mechanisms can effectively conserve N in soil under saturated conditions compared to unsaturated conditions in subtropical China. Biol. Fertil. Soils 54, 495–507.

Zhu, X., Burger, M., Doane, T.A., Horwath, W.R., 2013. Ammonia oxidation pathways and nitrifier denitrification are significant sources of N2O and NO under low oxygen availability. Proc. Natl. Acad. Sci. U. S. A. 110, 6328–6333.

Zhu, Y., Chen, Y., Ali, M.A., Dong, L., Wang, X., Archontoulis, S. V., Schnable, J.C., Castellano, M.J., 2021. Continuous in situ soil nitrate sensors: The importance of high-resolution measurements across time and a comparison with salt extraction-based methods. Soil Sci. Soc. Am. J. 85, 677–690.